

Analysis of Arrester Energy for 132kV Overhead Transmission Line due to Back Flashover and Shielding Failure

Nor Hidayah Nor Hassan^{1,a}, Ab. Halim Abu Bakar^{2,b}, Hazlie Mokhlis¹, Hazlee Azil Illias¹

¹Department of Electrical Engineering, Faculty of Engineering, University of Malaya, 50603 Kuala Lumpur, Malaysia

²UM Power Energy Dedicated Advanced Center (UMPEDAC), Level 4, Wisma R&D, University of Malaya, Jalan Pantai Baharu, 59990 Kuala Lumpur, Malaysia

^ahidayahassan@siswa.um.edu.my, ^ba.halim@um.edu.my

Abstract—This paper presents the analysis of lightning arrester energy due to back flashover and shielding failure phenomena in a 132kV transmission line in Malaysia. The transmission line, towers and surge arresters were modeled using PSCAD/EMTDC software. The model has been used to simulate the discharged energy from lightning arresters that were installed on the tower in the event of back flashover and shielding failure. The arrester was modeled based on the IEEE frequency dependent model. Comparison between the simulation results and values calculated theoretically was performed to validate the model that has been developed. The results show that both are in reasonable agreement with each other. The maximum calculated and simulated energy discharged by the arrester is found to be less than 5.1 kJ/kV, which is the rating of arresters installed in the actual 132kV transmission lines.

Keywords—Arrester; Back Flashover; Shielding Failure; Bergeron model; PSCAD/EMTDC

I. INTRODUCTION

Generally, the use of line arrester is to decrease or eliminate lightning flashover on transmission and distribution lines [1]. The purpose of line arrester installation in transmission line system is to improve the performance of overhead lines with poor shielding or with very high tower footing impedance [2]. Arresters avoid lightning flashovers since transmission lines insulation voltage is higher than the residual voltage developed across the arresters, either due to back flashover or shielding failure. However, the arresters have to withstand the energy discharged by the lightning stroke.

Shielding failure occurs when lightning strikes less than or equal to 20 kA bypass the overhead ground wires [3]. It is always designed such that overhead ground wires are located at a position which provides the least shielding failure. Thus, the majority of the lightning will terminate on the ground wires and build up a voltage across the line insulation. Back flashover will occur when these voltages exceed the line critical flashover (CFO). This paper presents the application of PSCAD software to estimate the arrester energy due to shielding failure (SF) and back flashover (BFO) phenomena. The ranges of the current stroke used in the simulation, which contributes to both phenomena, are stated in [3].

The CIGRE simulation method for 132kV has been developed and the arrester was based on the frequency

dependent model, which is represented with IEEE two sections of nonlinear resistance. Since the Maximum Continuous Operating Voltage (MCOV) of 132 kV transmission line is 97.2 kV, RVLQD - Class 2 type of arrester has been chosen because the rated voltage is between 3kV to 198kV as in the datasheet of porcelain type surge arrester from Toshiba.

II. MODELLING

The overhead lines are represented by multi-phase model, which consider the distributed nature of the line parameters due to the range of frequencies involved. Phase conductors and shield wires are modeled in detail between the towers. PSCAD/EMTDC was used to model transmission line, towers and surge arresters.

PSCAD/EMTDC was used because it offers real time analysis simulation. This software allows user to construct complex nonlinear power system models that combine three main components of a power system, power electronics and control circuits into one using more than 280 flexible components in the master library. Furthermore, PSCAD/EMTDC is suitable for simulating time domain instantaneous responses or electromagnetic transients for both electrical and control systems.

A. Transmission Line and Tower Model

Transmission line is modelled based on standard single circuit line geometry drawings and conductor data of a typical 132kV line. The transmission towers are represented geometrically similar to that of the single-storey lattice tower as shown in Figure 1. The lowest conductor from the ground is 16.45 m and the span length of the transmission line is 300m. Line geometry for the tower configuration is shown in Figure 2. The surge propagation velocity is assumed equal to 85% of the speed of light [4].

There are several formulae to calculate the surge impedance of the tower. As a basis, (1), which is for 'waist tower shape' [5] and recommended by IEEE and CIGRE [6] is used,

$$Z_t = 60 \ln [\cot \{0.5 \tan^{-1}(r_{avg}/h)\}] \quad (1)$$

where,

$$r_{avg} = \frac{r_1 h_1 + r_2 h + r_3 h_2}{h} \quad (2)$$

r_{avg} = equivalent radius of the tower represented by a truncated cone

h = tower height, m

h_1 = tower height from midsection to top, m

h_2 = tower height from base to midsection, m

r_1, r_2, r_3 = tower top, midsection and base radii, m

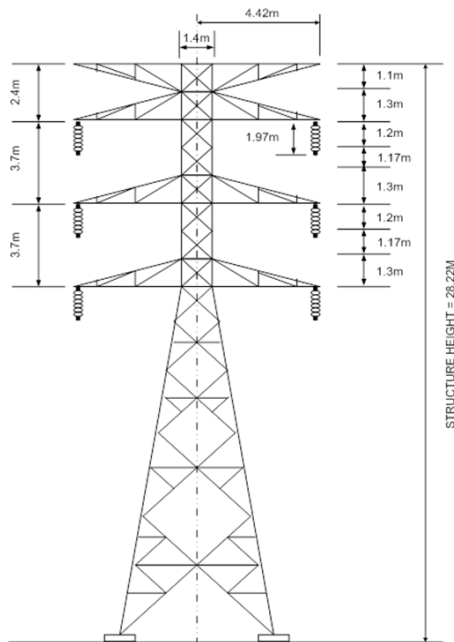


Figure 1. 132 kV tower dimension

General Line Geometry Data Input

Tower: 3H5 Tower Centre 0 [m]
 Conductors: Batang Ground_Wires: OPGW

Cond. #	Connection Phasing #	X (from tower centre)	Y (at tower)	GW. #	Connection Phasing #	X (from tower centre)	Y (at tower)
1	3	-4.42 [m]	23.85 [m]	1	1	-4.42 [m]	28.22 [m]
2	4	-4.42 [m]	20.15 [m]	2	2	4.42 [m]	28.22 [m]
3	5	-4.42 [m]	16.45 [m]				

Mid-Span Sag:
 5 [m] for Conductors
 3 [m] for Ground Wires

Ground Resistivity: 300.0 [ohm*m]
 Relative Ground Permeability: 1.0
 Earth Return Formula: Analytical Approximation

Figure 2. 132kV tower configuration

Five transmission towers were modelled as single conductor distributed parameter line (Bergeron model travelling wave) segments of 'transmission lines' in PSCAD, as shown in Figure 3. Since the line parameters are constant at the chosen frequency when the Bergeron model is used, the user may select the R, L and C values. Line termination at each side of the model is necessary to avoid any reflection that might affect the simulated overvoltages around the point of impact [7].

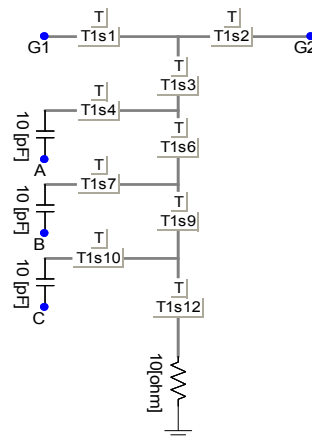


Figure 3. PSCAD tower model

B. Insulator String Model

The insulator is modeled as a stray capacitor (C) connected in parallel with a voltage controlled switch (S) as shown in Figure 4. The string which consists of glass insulators, provides an equivalent capacitance used in the model. Insulator supports the conductor by providing mechanical support that depends on its normal operating and transient voltage. The voltage withstand capability of the insulator is calculated using

$$V_o = 0.9(400 + \frac{710}{t^{0.75}})d \quad (3)$$

where,

V_o = flashover voltage, kV

t = time elapsed after lightning stroke, μ s [8, 9]

d = length of gap between arc horn, m

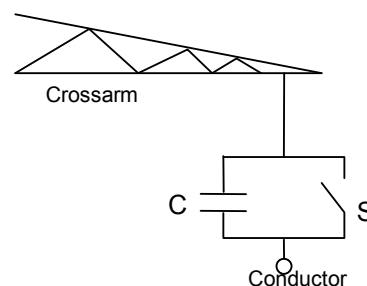


Figure 4 Insulator string flashover model

C. Line Arrester Model

The line arrester characteristics used in the simulation are shown in Table 1.

TABLE I. ARRESTER CHARACTERISTICS

Nominal voltage(kV)	120
MCOV(kV rms)	97.2
Voltage(kV) for 10 kA, 8/20 μ s	330
Energy absorption(kJ/kV)	4.5
Length of arrester column(m)	1.485
No. of parallel column of disks	1

The non-linear characteristic of the line arrester is modeled as recommended by the IEEE W.G 3.4.11, which is metal oxide surge arrester [10]. IEEE line arrester model has been chosen because the Toshiba surge arrester uses non linear resistor metal oxide elements as the main component. The frequency-dependent model consists of two non-linear resistors, A_0 and A_1 , which are separated by an R-L filter, as shown in Figure 5. Figure 6 shows the V-I characteristics of A_0 and A_1 obtained from 8/20 μs impulse data, which is supplied by the manufacturer.

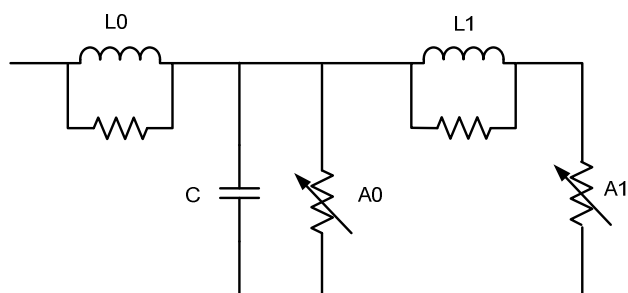


Figure 5: IEEE frequency-dependent model line arrester

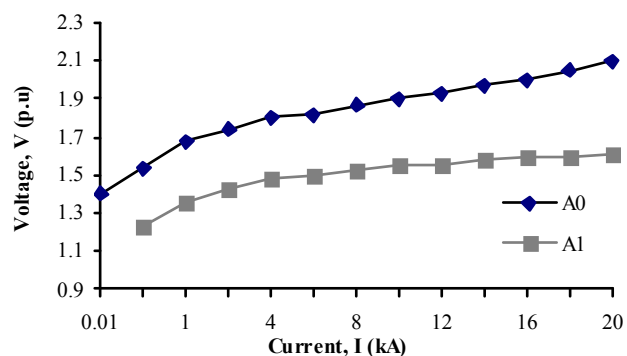


Figure 6: V-I non-linear characteristic for A_0 and A_1

The initial parameters of the resistor and inductor are calculated based on the estimated height of the arrester and the number of parallel columns of metal-oxide disks using [10]

$$L_1 = 15d / n \quad (\mu\text{H}) \quad (4)$$

$$R_1 = 65d / n \quad (\Omega) \quad (5)$$

$$L_o = 0.2d / n \quad (\mu\text{H}) \quad (6)$$

$$R_o = 100d / n \quad (\Omega) \quad (7)$$

$$C = 100n / d \quad (\text{pF}) \quad (8)$$

where,

d = estimated height of the arrester (as in data sheet), m

n = number of parallel columns of metal oxide in the arrester

The values of A_0 , A_1 and L_1 have to be adjusted so that the discharge voltages between theory and experiment have a good match.

III. LIGHTNING

The lightning source is modeled based on the IEC triangular wave shape, as shown in Figure 7 [11]. The lightning stroke is modeled by a current source in parallel with a lightning - path impedance, as shown in Figure 8. The lightning-path impedance is represented as a parallel resistance of 400 Ω [12]. A peak current source of different magnitudes has been used to investigate the effects of shielding failure (SF) and back flashover (BFO) phenomena on the arrester discharge energy. Table 2 shows the injected single stroke current for simulation of SF and BFO.

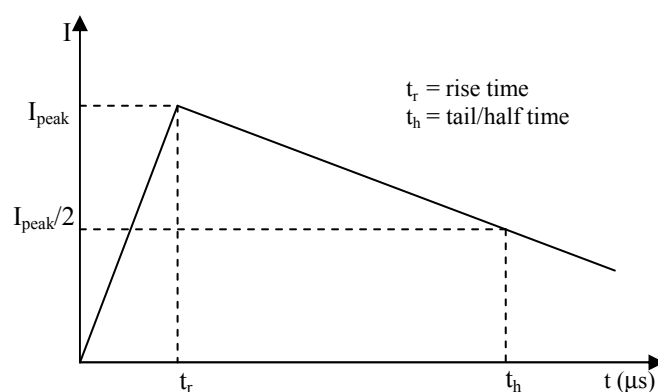


Figure 7: Recommended IEC triangular wave shape [11]

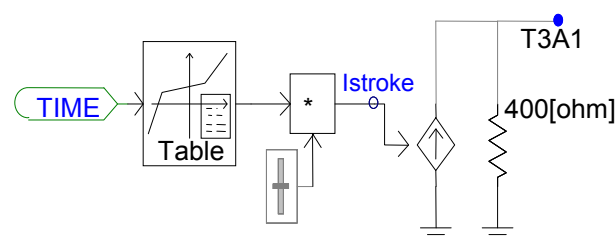


Figure 8: Lightning source model consisting of a current source and lightning path impedance

TABLE II. INJECTED CURRENT FOR SIMULATION

Injected Current, I (kA)	
BFO	SF
35	5
80	10
100	13
150	15
180	18
200	20

Transmission shielding failure and back flashover were simulated by injecting single stroke currents to a line phase conductor or ground wire of the third tower. The time to rise, t_r and time to half, t_f , are chosen as 8 μs and 20 μs .

IV. ARRESTER ENERGY

A. Stroke to Tower or Ground Wire

The energy discharged by the line arrester, W_A , during back flashover can be estimated using [1]

$$W_A = i_A e_A \tau \quad (9)$$

where,

- i_A = arrester current, A
- e_A = arrester discharge voltage, V
- τ = time constant, s

The time constant of the arrester current, τ , is estimated by

$$\tau = \frac{Z_g}{R_i} T_s \quad (10)$$

where,

- Z_g = ground wire impedance, Ω
- R_i = footing resistance, Ω
- T_s = span length divided by the velocity of light, s

B. Stroke to Phase Conductor

Lightning that struck at the phase conductor will give a different estimation of arrester energy discharged from lightning that struck at ground wire. The energy discharged by the surge arrester, W_A , during shielding failure can be expressed as an integral form of product of arrester current and discharge voltage [1].

$$W_A = \int_0^{\infty} i_A e_A dt \quad (11)$$

The relation between the arrester current and discharge voltage can be represented by [13]

$$i_A = k(e_A)^\alpha \quad (12)$$

Combining both equation (11) and (12), simple arrester discharge energy equation can be express by

$$W_A = \frac{K_1 I_{e_{A1}} \tau_1}{1 + 1/\alpha} \quad (13)$$

where E_{A1} are the discharge voltage for current of $K_1 I$ and α is $-t / \tau_1$. Detailed derivation of both equations is explained in [1].

V. RESULTS AND DISCUSSION

In practice, the 132kV transmission lines are equipped with 5.1kJ/kV energy of surge arrester. Thus, comparisons between the calculation and simulation was performed for:

- a) back flashover for stroke current range of 20 kA to 200 kA
- b) shielding failure for stroke current range of 0 kA to 20 kA

Over 50% of the lightning strokes contain more than one stroke, which is also known as multiple strokes lightning (MSL) [14]. However, in this work, single stroke lightning (SSL) current magnitude was only considered.

A. Stroke to Tower or Ground Wire

The stroke current strikes directly to ground wire or tower, creating back flashover phenomena. Figure 9 shows the voltage across the arrester when a lightning current of 20 kA, 8/20 μ s was injected on the third tower.

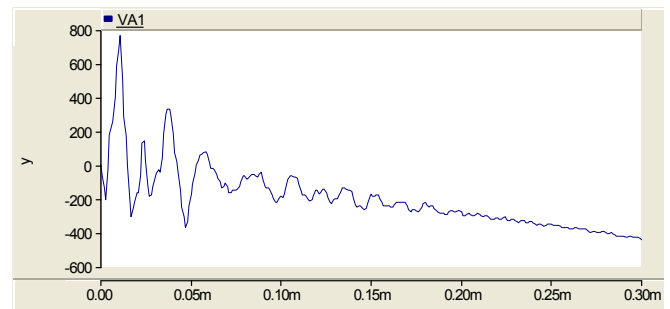


Figure 9: Voltage across arrester for 20 kA stroke to the ground wire

The energy dissipated by the frequency dependent model, which consists of two non-linear resistors, A_0 and A_1 are shown in Figures 10 and 11. The total of these energies discharged by the line arrester is shown in Figure 12.

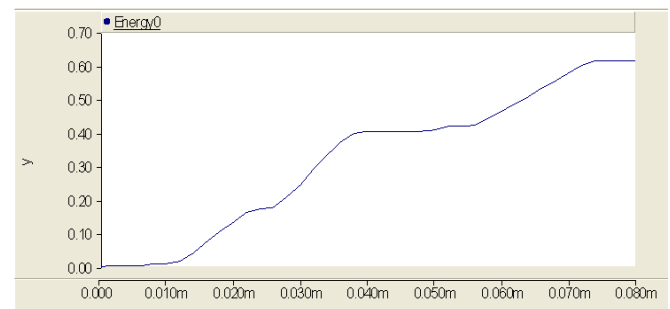


Figure 10: A_0 energy waveform for 20 kA stroke to the ground wire

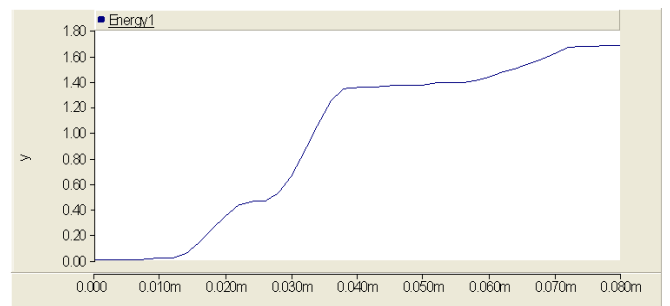


Figure 11: A_1 energy waveform for 20 kA stroke to the ground wire

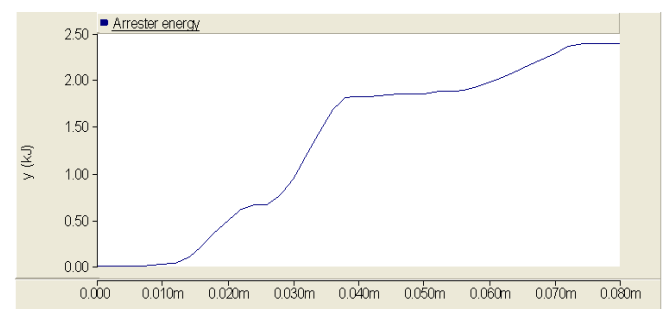


Figure 12: Simulated energy discharged by the line arrester for 20 kA stroke to the ground wire

Table 3 and Figure 13 show comparison between the calculated energy values using (9) and the values obtained from simulation results of stroke currents between 20 kA to 200 kA. It was found that the simulated energy is slightly different than the calculated energy. This might due to the transmission line parameter used for tower models in the simulation are inaccurate.

TABLE III. ENERGY OF ARRESTER DURING BACK FLASHOVER

Stroke Current (kA)	Calculated Energy (kJ/kV)	Simulated Energy (kJ/kV)
35	0.06	0.07
80	0.15	0.24
100	0.25	0.31
150	0.50	0.52
180	0.65	0.64
200	0.76	0.73

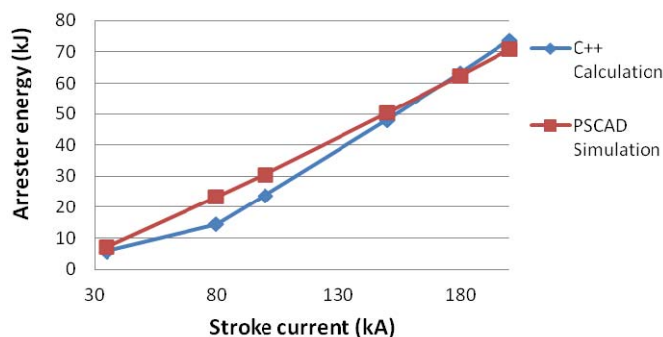


Figure 13: Comparison of arrester energy during back flashover

B. Stroke to Phase Conductor

A direct lightning stroke to phase conductor may result in a shielding failure. This occurs when lightning currents of less than or equal to 20kA bypass the overhead shield wire. For this case, only SSL current magnitudes of 5kA to 20kA were simulated because shielding failures tend to occur between these values. The designed line arrester was placed at the top phase A_1 of the third tower and different SSL currents were injected at the top phase conductor.

The waveform of the discharge voltage across the phase A_1 when a 20kA lightning stroke terminates at the top conductor is shown in Figure 14.

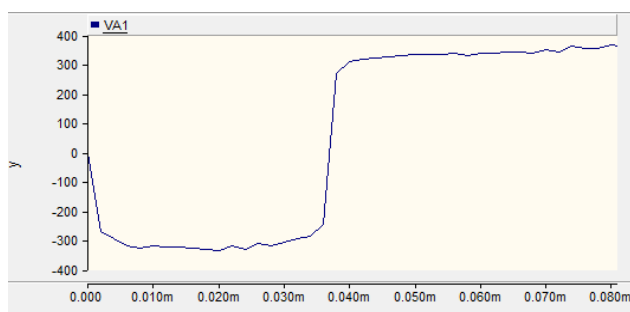


Figure 14: Voltage across surge arrester for 20 kA stroke to phase conductor

The energy discharged by the non-linear element of A_0 and A_1 obtained from the simulation when the peak current magnitude was injected to the conductor is shown in Figures 15 and 16.

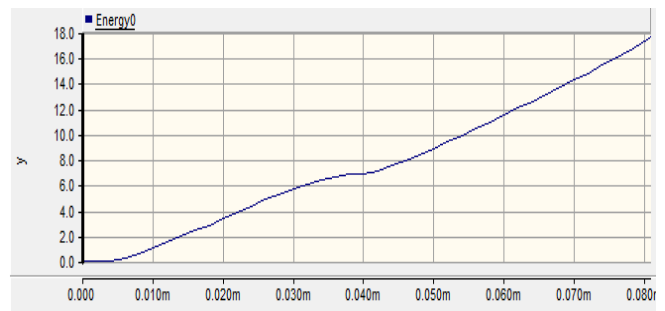


Figure 15: A_0 energy waveform for 20 kA stroke to phase conductor

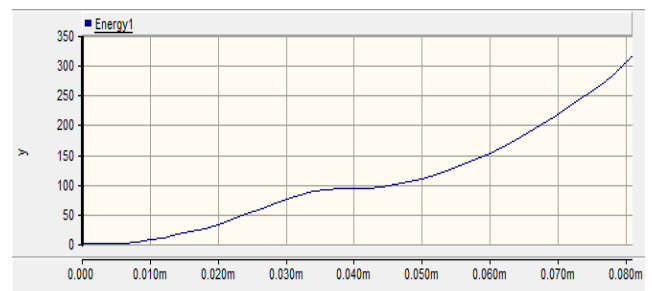


Figure 16: A_1 energy waveform for 20 kA stroke to phase conductor

Both A_0 and A_1 do not share the discharge energy equally because of the inductance between the elements. The sum of the two energy results in the total energy absorption of the line arrester due to shielding failure is shown in Figure 17.

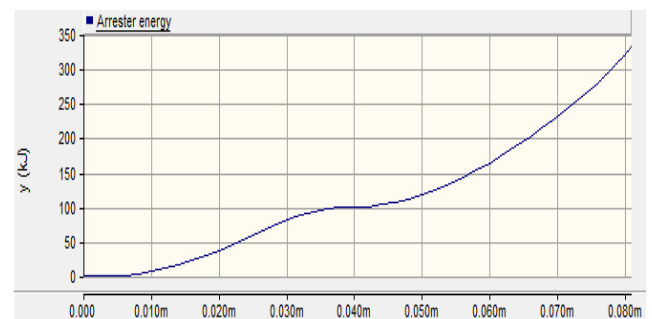


Figure 17: Simulated energy discharged by the line arrester for shielding failures

To calculate the arrester energy analytically, the stroke current is assumed to have exponential tail decay. The time to half value of the stroke current is chosen as $20\mu\text{s}$, hence the tail time constant, τ , is $29\mu\text{s}$. Assuming the arrester discharges the entire stroke current, the energy dissipated can be calculated from (10) and (11). Figure 18 shows comparison between the calculated and simulated results of the arrester discharge energy in kJ due to SSL striking the top phase conductor.

Table 4 summarizes the results of the obtained total energy dissipated by the arrester in kJ/kV of MCOV for different peak current magnitudes. Increase in the lightning current results in a higher energy discharged by the arrester.

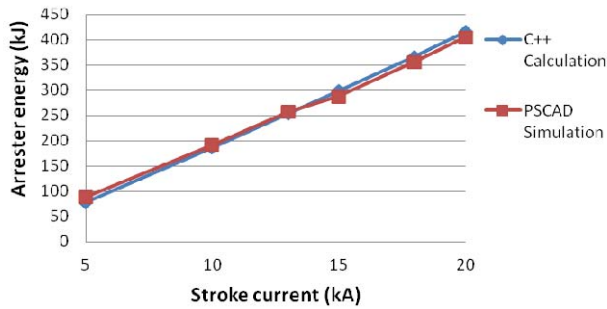


Figure 18: Comparison of arrester energy during shielding failure

TABLE IV. ENERGY OF ARRESTER DURING SHIELDING FAILURE

Stroke Current (kA)	Calculated Energy (kJ/kV)	Simulated Energy (kJ/kV)
5	0.80	0.91
10	1.92	1.97
13	2.61	2.65
15	3.08	2.96
18	3.78	3.67
20	4.28	4.16

C. Effect of footing resistance

The effect of the footing impedance was analyzed by assuming a simple linear resistance for its model. Table V shows the energy discharged through the arrester installed at phase "A" of the test line as a function of the tower footing resistance for both back flashover and shielding failure. Note that, as the footing resistance increases, energy discharged for lightning that strikes to the ground wire also increases. For lightning strikes at phase conductor, arrester energy remains the same as the footing resistance increases. Therefore, any changes to the footing resistance does not change the energy of arrester for shielding failure phenomena. This situation differs for back flashover phenomena as the energy discharged increases if the footing resistance increases.

TABLE V. ENERGY OF ARRESTER FOR DIFFERENT FOOTING RESISTANCE

Rf, Ω	Energy, kJ/kV	
	Current 200 kA at ground wire (Back flashover)	Current 18 kA at phase A (Shielding Failure)
10	0.7296	3.67
20	0.7353	3.67
30	0.7390	3.67
40	0.7417	3.67
50	0.7454	3.67
60	0.7530	3.67

VI. CONCLUSION

The work in this paper has investigated the capability of the arresters installed in 132 kV transmission lines in

Malaysia, in withstanding single stroke lightning discharged energy caused by shielding failure and back flashover phenomena. The arrester energy discharged due to shielding failure and back flashover was calculated using analytical method and simulation using PSCAD/EMTDC. Comparison between the simulation results and values calculated theoretically shows that both results are within reasonable agreement to each other. The effect of footing resistance to the energy discharged also been covered in this paper. Only back flashover phenomena will increase the energy discharged as the footing resistance increases. The rating of the arresters installed in the actual 132kV transmission lines, which is 5.1 kJ/kV, has been found capable of handling the maximum energy discharged by the designed arrester. Future work will consider other current impulse wave shape and multiple strokes lightning to study the behavior of arrester energy.

ACKNOWLEDGMENT

The author thanks the University of Malaya for supporting this work through the IPPP research grant (Grant no: PS012-2012A).

REFERENCES

- [1] A. R. Hillman, "Insulation Coordination for Power Systems," Marcel Dekker, 1999.
- [2] CIGRE WG 33.11, "Application of Metal Oxide Surge Arresters to Overhead Lines," *Electra*, October 1999.
- [3] C.A. Nucci, "A Survey on Cigré and IEEE Procedures for the Estimation of the Lightning Performance of Overhead Transmission and Distribution Lines," in *Asia-Pacific International Symposium on Electromagnetic Compatibility (APEMC)*, Beijing, pp. 1124-1133, 2010.
- [4] IEEE Working Group, "A Simplified Method for Estimating Lightning Performance of Transmission Lines," *IEEE Trans. Power App. Syst.*, vol. PAS-104, no. 4, pp. 919-932, Apr. 1985.
- [5] W.A. Chisholm, Y.L. Chow, K.D. Srivastava, "Travel Time of Transmission Towers," *IEEE Trans. on Power Apparatus and Systems*, vol. 104, no. 10, pp. 2922-2928, October 1985.
- [6] CIGRE WG 33.01, "Guide to Procedures for Estimating the Lightning Performance of Transmission Lines," *CIGRE Brochure 63*, 1991.
- [7] Juan A. Martinez-Velasco, Castro-Aranda, "Modeling of Overhead Transmission Lines for Lightning Studies," *IPST'05 in Montreal, Canada No. IPST05 - 190*, June 19-23, 2005.
- [8] IEEE Standard, "IEEE Guide for Improving the Lightning Performance of Transmission Lines", *IEEE Std* pp. 1243-199.
- [9] D. Caulker, A. Hussein, Z.A. Malek, S. Yusof, "Shielding Failure Analysis of 132 kV Transmission Line Shielded by Surge Arresters Associated with Multiple Strokes Lightning," *International Conference on Electrical and Computer Engineering (ICECE)*, 2010, vol., no., pp.298-301, 18-20 Dec. 2010.
- [10] IEEE WG 3.4.11, "Modelling of Metal Oxide Surge Arresters," *IEEE Trans. On Power Delivery*, vol. 7, pp.302-309, Jan. 1992.
- [11] A.H.A. Bakar, H. Mokhlis, A.L. Lim, W.P. Hew, "Lightning Over voltage performance of 132kV GIS Substation in Malaysia," *International Conference on Power System Technology (POWERCON), 2010*, vol., no., pp.1-7, 24-28 Oct. 2010.
- [12] A. Ametani, T. Kawamura, "A Method of a Lightning Surge Analysis Recommended in Japan Using EMTF," *IEEE Trans. on Power Delivery*, Vol. 20, No. 2, pp. 867-875, April 2005.
- [13] T. E. McDermott, D. E. Parrish, and D. B. Miller, *Lightning Protection and Design Workstation Seminar Notes*, EPRI TR-000530, Sep. 1992.
- [14] PSCAD/EMTDC Manual, "Introduction to PSCAD/EMTDC V3", Manitoba HVDC Research Centre Inc. 2001.